CHEMISTRY
A EUROPEAN JOURNAL

ChemPubSoc
Europe

DOI: 10.1002/chem.201201665

# Experimental and Theoretical Evidence for Multiple $Fe^{IV}$ Reactive Intermediates in TAML-Activator Catalysis: Rationalizing a Counterintuitive Reactivity Order**

**Soumen Kundu, Medini Annavajhala, Igor V. Kurnikov,* Alexander D. Ryabov,* and Terrence J. Collins*[a]**

TAML activators **1a** and **1b** (Figure 1 A) are both faithful mimics of the peroxidase- and short-circuited cytochrome P450 enzymes and exceptional homogeneous oxidation catalysts.[1,2] Upon oxidation by primary oxidants, TAML systems form multiple $Fe^{IV}$ and $Fe^{V}$ reactive species. For example, following oxidation of **1a** by *meta*-chloroperbenzoic acid (*m*CPBA), the first $Fe^{V}O$ coordination complex could be trapped at low temperature and fully authenticated.[3] In non-coordinating solvents, compound **1a** reacts with $O_2$ to form a μ-oxo-$(Fe^{IV})_2$ species.[4] Complex **1a** is also oxidized by $H_2O_2$ or *t*BuOOH in water to form either a mono-oxo-$Fe^{IV}$ complex (pH > 12) or the aforementioned μ-oxo-$(Fe^{IV})_2$ complex (pH < 10) and these are inter-related by a pH dependent equilibrium.[5,6] Direct kinetic analyses of the formation of μ-oxo-$(Fe^{IV})_2$ are consistent with the initial formation of $Fe^{V}O$ followed by its comproportionation with $Fe^{III}$.[7] Characterization of these high-valent iron complexes has been supported by mass spectrometry and structural techniques (X-ray- and extended X-ray absorption fine structure (EXAFS) spectroscopies), but the precise definition of atomic-electronic structures provided by Mössbauer and EPR spectroscopies in combination with DFT has been vital throughout. Integer spin EPR ($Fe^{IV}$) spectroscopy and Mössbauer spectroscopy ($Fe^{IV}$, $Fe^{V}$) both require a relatively high TAML concentration (0.1–1 mM),[3,6] which limits their use during catalysis where the TAML concentrations (0.01–1 μM) are much lower. Moreover, extrapolation of the reactivity results from stoichiometric to catalytic studies is not possible because the overall TAML concentration influences the speciation among $Fe^{III}$, $Fe^{IV}$, and $Fe^{V}$ which, in turn, affects the reactivity.[8] With decreasing TAML concentration in water, the $Fe^{IV}$ species change from dimers (> 1 μM) to monomers (< 1 μM), which substantially alters the rates of substrate oxidations.[8] Thus, we required alternative approaches for characterizing the reactive species during fast catalysis to better map the catalyst reactivity landscape. In this contribution, we show how to use chemical kinetics to obtain evidence for the likely structures and behavior of multiple monomeric $Fe^{IV}$ intermediates during the $H_2O_2$ oxidation of ferrocyanide to ferricyanide that is catalyzed by **1a** and **1b** (Figure 1 B). Furthermore, by partnering the kinetic results with ab initio calculations, we have been able to rationalize the otherwise counterintuitive comparative reactivity of the different $Fe^{IV}$ species.

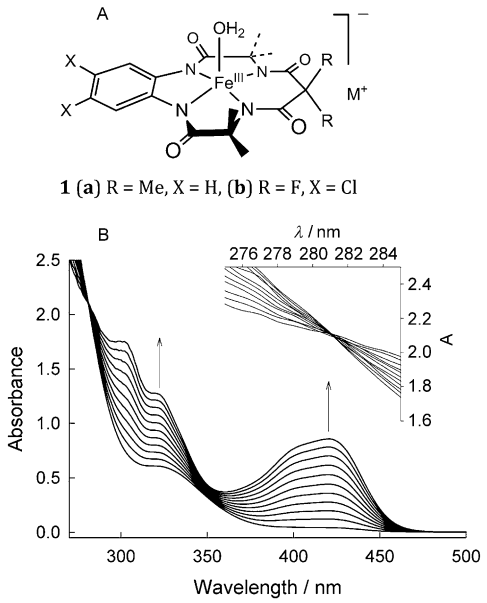


Figure 1. A) TAML activators employed: M = Na (**1a**), Li (**1b**). B) Spectral changes associated with the catalytic oxidation of $[Fe(CN)_6]^{4-}$ to $[Fe(CN)_6]^{3-}$ by **1a**/$H_2O_2$. Data was collected every 20 s. The arrows indicate the formation of $[Fe(CN)_6]^{3-}$. Conditions: $[\mathbf{1a}] = 1.68\times10^{-7}$ M, $[H_2O_2] = 2.4\times10^{-3}$ M, $[[Fe(CN)_6]^{4-}] = 1.5\times10^{-3}$ M, 0.01 M phosphate buffer, pH 10, 25 °C. Inset: Isosbestic point at 281 nm indicative of a selective transformation of $[Fe(CN)_6]^{4-}$ to $[Fe(CN)_6]^{3-}$.

TAML-activator-catalyzed oxidation of conventional dyes by $H_2O_2$ does not normally follow monoexponential kinetics

[a] S. Kundu, M. Annavajhala, Prof. I. V. Kurnikov, Prof. A. D. Ryabov, Prof. T. J. Collins
Department of Chemistry
Carnegie Mellon University
4400 Fifth Avenue, Pittsburgh, PA 15213 (USA)
Fax: (+1) 412-268-1061
E-mail: igor@kurnikov.org
ryabov@andrew.cmu.edu
tc1u@andrew.cmu.edu

[**] TAML = tetra-amido macrocyclic ligand

Supporting information for this article is available on the WWW under http://dx.doi.org/10.1002/chem.201201665.

under pseudo-first order conditions. This catalytic feature is kinetically well-understood.[1,9–11] The non-exponential behavior may partly be due to the intra-molecular deactivation of the catalyst under operating conditions.[11] Hence, initial or steady-state rates were measured for characterization of the catalytic activity of TAML activators.[1,10] The reported kinetic data has been interpreted in terms of the general mechanism shown in Scheme 1.[10] The TAML activator is

$$Fe^{III}\text{-TAML} + H_2O_2 \underset{k_{-I}}{\overset{k_I}{\rightleftharpoons}} (\text{Oxidized TAML})$$
$$(\text{Oxidized TAML}) + Fe(CN)_6^{4-} \xrightarrow{k_{II}} Fe^{III}\text{-TAML} + Fe(CN)_6^{3-}$$

Scheme 1. General mechanism of the catalytic oxidation of $[Fe(CN)_6]^{4-}$ to $[Fe(CN)_6]^{3-}$ by TAML Activator.

reversibly oxidized by $H_2O_2$ ($k_1$, $k_{-1}$) to form "Oxidized TAML", which then converts ferrocyanide to ferricyanide ($k_{II}$). Under steady-state conditions, the reaction rate is expressed by Equation (1), which has been derived by applying the steady-state approximation to "Oxidized TAML" while using the mass balance equation for the catalyst $[Fe^{III}]_t = [Fe^{III}\text{–TAML}] + [\text{Oxidized TAML}]$. The $k_{-I}$ in Equation (1) is negligible compared with $k_I[H_2O_2] + k_{II}[Fe(CN)_6^{4-}]$.[10] Equation (1) also shows why the reaction should not follow exponential kinetics. In fact, if $k_{II}[Fe(CN)_6^{4-}] \gg k_I[H_2O_2]$, $Rate = k_I[H_2O_2][Fe^{III}]_t$ and the reaction is formally zero-order in ferrocyanide. Equation (2) is obtained upon rearrangement of Equation (1).

$$Rate = \frac{k_I k_{II}[H_2O_2][[Fe(CN)_6]^{4-}][Fe^{III}]_t}{k_{-I} + k_I[H_2O_2] + k_{II}[[Fe(CN)_6]^{4-}]} \quad (1)$$

$$\frac{[Fe^{III}]_t}{Rate} = \frac{1}{k_I[H_2O_2]} + \frac{1}{k_{II}[[Fe(CN)_6]^{4-}]} \quad (2)$$

In previous studies, a strong dependency of $k_I$ on the pH was discovered and found to originate in the Brønsted acid behavior of an axial water ligand on iron and the peroxide.[1,12] Naturally, we wanted to know if $k_{II}$ is pH sensitive. Thus, **1a** and **1b** catalyzed oxidations of ferrocyanide by $H_2O_2$ were studied in buffered aqueous medium covering the pH range of 7 to 12. Ferrocyanide is an ideal substrate (see the Supporting Information) because it is tetra-anionic ($[Fe(CN)_6]^{4-}$) across this pH range[13] such that any variations in $k_{II}$ would be attributable to changes in the speciation of "Oxidized TAML".[14]

Upon examination at every integer pH value, the reaction rate was found to depend linearly on the catalyst concentration ($[Fe^{III}]_t$) over a wide range (0.01–0.5 μM) (see Figure 2S in the Supporting Information) and to pass through the origin, which is consistent with Equation (1). The reaction rate increases hyperbolically with increasing peroxide and ferrocyanide concentrations (Figure 2A and B), as required by Equation (1). The inverse of the rate varies linearly with the inverse of the concentrations for peroxide and substrate (see insets of Figure 2A and B). The rate constants $k_I$ and

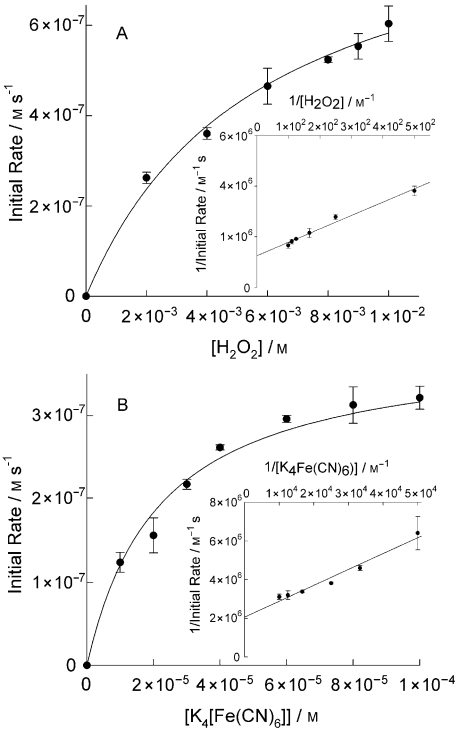


Figure 2. Initial rates of the oxidation of $[Fe(CN)_6]^{4-}$ to $[Fe(CN)_6]^{3-}$ by **1b**/$H_2O_2$ as a function of $[H_2O_2]$ (A) and $[K_4[Fe(CN)_6]]$ (B). Insets: Double reciprocal plots of the initial rates as a function of $[H_2O_2]$ (A) and $[K_4Fe(CN)_6]$ (B). Conditions: A) $[K_4Fe(CN)_6] = 2\times10^{-4}$ M, **[1b]** $= 5\times10^{-8}$ M; B) $[H_2O_2] = 6\times10^{-3}$ M, **[1b]** $= 5\times10^{-8}$ M; 0.01 M phosphate buffer, pH 9, 25 °C.

$k_{II}$ could then be calculated from the slopes and intercepts of these inset graphs [Eq. (2)]. For the $[H_2O_2]$ variation, $k_I = 3\times10^3\,M^{-1}s^{-1}$ and $k_{II} = 5\times10^5\,M^{-1}s^{-1}$. For the $[[Fe(CN)_6]^{4-}]$ variation, $k_I = 2.5\times10^3\,M^{-1}s^{-1}$ and $k_{II} = 4\times10^5\,M^{-1}s^{-1}$. Thus, comparable values of $k_I$ and $k_{II}$ arise from the variation of peroxide and substrate concentrations supporting the validity of exercising the steady-state assumption. Moreover, the calculated $k_I$ value ($2\times10^3\,M^{-1}s^{-1}$, pH 9, **1a**) is in good agreement with the value reported in prior work for oxidation of a separate substrate, Orange II dye ($1.4\times10^3\,M^{-1}s^{-1}$, pH 9, **1a**).[10] As with other synthetic catalysts[15] and unlike peroxidase enzymes,[16] the peroxide activation step ($k_I$) for the TAML activators is usually slower than the substrate oxidation ($k_{II}$).[1,11] It is noteworthy that in this study, a change in the rate-determining step was observed as the pH was varied (see the Supporting Information). Between the pHs 7 and 8, $k_I[H_2O_2] < k_{II}[[Fe(CN)_6]^{4-}]$ and as a consequence the reaction rate is linearly dependent on $[H_2O_2]$ below $1.5\times10^{-3}$ M and independent of $[[Fe(CN)_6]^{4-}]$ (see Figure 3S in the Supporting Information), indicative of the rate law being transformed to $Rate = k_I[H_2O_2][Fe^{III}]_t$. To measure $k_{II}$,

  

a much higher $H_2O_2$ concentration (relative to the concentrations used to produce Figure 2; inset of Figure 3S A in the Supporting Information) was used, so that the terms $k_I$-$[H_2O_2]$ and $k_{II}[[Fe(CN)_6]^{4-}]$ are comparable. However, between pH 11 and 12, $k_I[H_2O_2] > k_{II}[[Fe(CN)_6]^{4-}]$ and as a consequence the reaction rate is independent of $[H_2O_2]$ and linearly dependent on $[[Fe(CN)_6]^{4-}]$ (see Figure 4S in the Supporting Information), indicative of the rate law $Rate = k_{II}[[Fe(CN)_6]^{4-}][Fe^{III}]_t$. The second-order rate constant $k_{II}$ was estimated from the slope of the straight line (see Figure 4S B in the Supporting Information).

Iron(III) TAML is oxidized to iron(IV) TAML[5] by $H_2O_2$ and can in principle be oxidized to $Fe^V$, because $H_2O_2$ is a 2e oxidant. The $Fe^VO$ species has been detected only in organic solvents at low temperature, but not yet in water at room temperature in which the $Fe^{IV}$ species are usually observed. Based upon the ability of TAML activators to rapidly oxidize recalcitrant organic molecules, a feat beyond the oxidizing potency of the various $Fe^{IV}$ intermediates, we believe that $Fe^VO$ is a critical fleeting intermediate in the catalytic cycles in water. Under catalytic as compared with stoichiometric conditions, the TAML activator concentration is much lower such that the reactivity of $Fe^VO$ is probably directed primarily at the substrate instead of at $Fe^{III}$, a hypothesis backed by the linear dependence of the reaction rate with $[Fe^{III}]_t$ (see Figure 2S in the Supporting Information). This is simply a reproduction of the familiar story of Compound I and II in peroxidase enzymes (see the Supporting Information for details).[14] In the studies below, we have not included $Fe^VO$ in our kinetic schemes because, even if it is present, it will be kinetically silent under the steady-state conditions due to its much higher reactivity ($10^4$-times faster) compared with a representative $Fe^{IV}$ TAML species.[7] A similar approach was adopted for the kinetic analysis of ferrocyanide oxidation by horseradish peroxidase Compound II, in which Compound I was only 40 times more reactive than Compound II.[14] Thus, the kinetic data for the oxidation of ferrocyanide by TAML/$H_2O_2$ is rationalized in Scheme 1 with the $Fe^{IV}$ TAML species as the "Oxidized TAML" under the assumption that $Fe^VO$ is kinetically silent.

For both catalysts **1a** and **1b**, the asymmetrical bell-shaped $k_{II}$ vs. pH profiles are observed (Figure 3). The simplest sequence of events that adequately accounts for the observed variation of $k_{II}$ with pH is shown in Scheme 2. The asymmetrical shape of the plot over the pH range of 7 to 12 with the presence of four plateaus indicates that four "Oxidized TAML" species (*A*–*D*) are involved in fast acid–base equilibria ($K_{a1}$–$K_{a3}$, Scheme 2). The data in Figure 3 are quantifiable in terms of Equation (3), which is derived assuming the elementary steps shown in Scheme 2. The values of the individual rate constants ($k_1$–$k_4$) and equilibrium constants ($K_{a1}$–$K_{a3}$) were obtained by the non-linear least squares analysis of the $k_{II}$ vs. pH plot. The best fit values of the parameters were used to generate the solid lines in Figure 3. The initial estimates of the rate and equilibrium constants were obtained by dividing the profile into three pH regions, in which only one pair of "Oxidized TAML" species dominates (see the Supporting Information), and then fitting the data to the corresponding modified equation (Equation (1S) in the Supporting information). The values of $k_1$ and $k_4$ (Table 1) have large errors because each makes only a minor contribution to the overall reactivity.

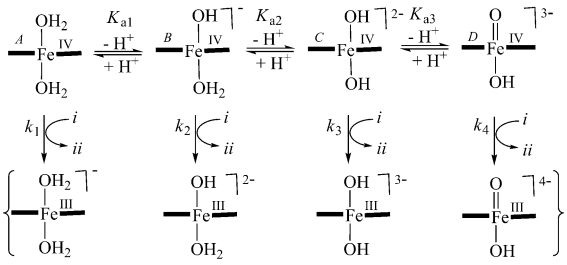


Scheme 2. Mechanism of oxidation of $[Fe^{II}(CN)_6]^{4-}$ to $[Fe^{III}(CN)_6]^{3-}$ by different "Oxidized TAML" intermediates *A*–*D*, which accounts for the pH profiles shown in Figure 3. Reduced TAML species are shown as used in the ab initio calculations; $i = [Fe^{II}(CN)_6]^{4-}$, $ii = [Fe^{III}(CN)_6]^{3-}$.

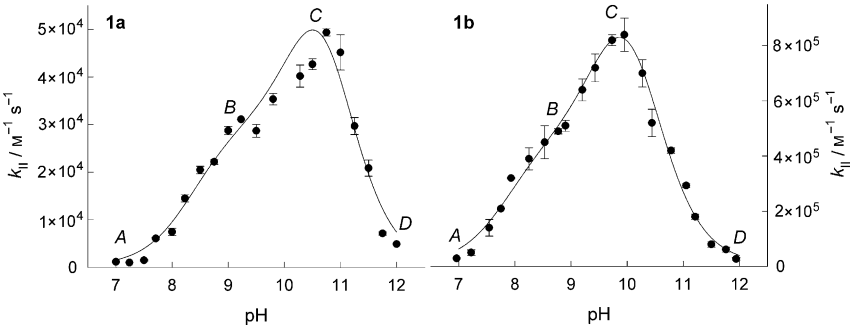


Figure 3. pH profiles of the rate constants $k_{II}$ (Scheme 1) for the oxidation of $[Fe(CN)_6]^{4-}$ to $[Fe(CN)_6]^{3-}$ by **1a**/$H_2O_2$ (left) and **1b**/$H_2O_2$ (right) (25 °C, 0.01 M phosphate buffer). *A*, *B*, *C*, and *D* are the dominant species (Scheme 2) at the indicated pH values. The solid line was calculated using the best fit values of $k_1$–$k_4$ and $K_{a1}$–$K_{a3}$ (Table 1, Scheme 2, see text for details).

$$k_{II} = \frac{k_1[H^+]^3 + k_2K_{a1}[H^+]^2 + k_3K_{a1}K_{a2}[H^+] + k_4K_{a1}K_{a2}K_{a3}}{[H^+]^3 + K_{a1}[H^+]^2 + K_{a1}K_{a2}[H^+] + K_{a1}K_{a2}K_{a3}} \quad (3)$$

Several significant points can be inferred from Scheme 2 and Table 1. First, **1b** is more reactive ($\approx$10 fold) than **1a** ($k_1$–$k_4$, Table 1). At pH 10 (maximum for **1b**, Figure 3) and 10.75 (maximum for **1a**) the $k_{II}$ values for **1b** and **1a** are $8.5\times10^5\,M^{-1}s^{-1}$ and $5\times10^4\,M^{-1}s^{-1}$, respectively. The presence of the electron-withdrawing halogen (Cl, F) atoms make **1b** more electrophilic and thus a more reactive electron-trans-

  

Table 1. Equilibrium and rate constants for the oxidation of ferrocyanide to ferricyanide by "Oxidized TAML" (Scheme 2, [Eq. (3)]).

| Catalyst | $k_1$ $[M^{-1}s^{-1}]$[a] | $k_2$ $[M^{-1}s^{-1}]$ | $k_3$ $[M^{-1}s^{-1}]$ | $k_4$ $[M^{-1}s^{-1}]$[a] | $pK_{a1}$ | $pK_{a2}$ | $pK_{a3}$ |
|---|---|---|---|---|---|---|---|
| **1a** | $\approx 3\times10^2$ | $(3\pm0.8)\times10^4$ | $(8.2\pm0.4)\times10^4$ | $\approx 0.5\times10^2$ | $8.3\pm0.3$ | $10.4\pm0.7$ | $11.0\pm0.4$ |
| **1b** | $\approx 5\times10^3$ | $(4.7\pm0.9)\times10^5$ | $(1.3\pm0.2)\times10^6$ | $\approx 1\times10^3$ | $7.8\pm0.3$ | $9.7\pm0.3$ | $10.4\pm0.2$ |

[a] Could not be more accurately estimated.

fer oxidant compared with **1a**. The higher reactivity of **1b** vs. **1a** has been previously reported[11,17] and **1b** has found wider application in the oxidative degradation of recalcitrant pollutants.[17–20] Prior to this contribution, the activating effects of electron-withdrawing groups on the TAML macrocycles could be rationalized by faster activation of hydrogen peroxide ($k_I$, Scheme 1).[1] However, the electron-withdrawing influence on $k_I$ has only been moderate to date. With the analysis presented here, we can now assert that electron-withdrawing groups on the macrocycles can produce large accelerations through $k_{II}$ across a wide pH range. Second, TAML activators are much more reactive in $k_{II}$ processes towards ferrocyanide than horseradish peroxidase Compound II in the pH range examined—$k_{II}$(HRP-Compound II) = $(0.24–4)\times10^3\,M^{-1}s^{-1}$ (pH 9.9–10.3). TAML activators also enjoy a large molecular weight advantage over the enzymes. Third, on iron(IV) the $pK_a$ values (Table 1) of the axial water ligands (*A* and *B*, Scheme 2) and hydroxide (*C*, Scheme 2) of **1b** are lower than those of **1a**, resulting from the higher electrophilicity at iron of **1b**. A similar trend has been observed for the experimentally determined $pK_a$ values of water on ferric TAML activators (10.1 for **1a** and 9.4 for **1b**).[21] TAML ligands with four deprotonated amides are significantly more electron-donating than porphyrins, which results in the much higher $pK_a$ values (9.4–10.5)[21] for the axial water in the ferric TAMLs compared to similar diaqua $Fe^{III}$-porphyrin complexes. For electron-rich and electron-deficient $Fe^{III}$-porphyrins, the $pK_a$ values of the axially coordinated water varies from 5.5 to 7.0.[22–24] Coordinated to iron(III), electron-donating $CN^-$ ligands decrease significantly the acidity of the axial water ($pK_a \approx 11–12$).[22]

Remarkably, the reactivity trend in the *A*–*D* series described by the rate constants $k_1$–$k_4$ is counterintuitive because deprotonation of metal-containing oxidants makes them more electron-rich implying that they should be less reactive in electron-transfer processes. But here the first two deprotonations (Scheme 2) make *B* and *C* more reactive than *A* (Table 1, Figure 3). Only the third deprotonation to form *D* results in a drop of reactivity (Table 1, Figure 3). To satisfy our troubled curiosity, we have analyzed the interesting trend theoretically using ab initio quantum chemical calculations for the water solvated $Fe^{IV}$-TAML and $Fe^{III}$-TAML species. From these calculations, the counterintuitive nature of the non-monotonic $k_{II}$ vs. pH profile can be explained because there are competing contributions to the overall free energy of electron-transfer arising from, on the one hand, the electronic effects associated with protonation/deprotonation of the TAML complexes (calculated in vacuo) and, on the other, from the relative solvation effects of the $Fe^{IV}$ and $Fe^{III}$ species at the various states of protonation (calculated in water) (Figure 4).

With progressive loss of protons, the $Fe^{IV}$ does indeed become less oxidizing as determined by the increasing

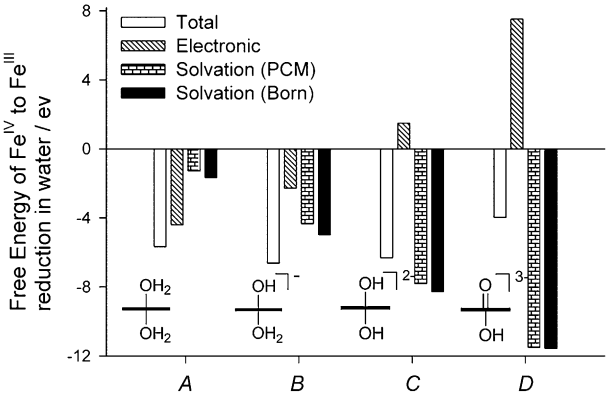


Figure 4. Contributions of electronic free energy in vacuum, solvation free energy [Polarizable Continuum Model (PCM) and Born model)] in water to the total free energy change (Electronic + Solvation PCM) for the reduction of $Fe^{IV}$ to $Fe^{III}$ TAML species (*A*-*D*, Scheme 2) in water.

$\Delta G_{electronic}$ term on going from *A* to *D* (see Figure 4 and the Supporting Information). The solvation energy changes can be qualitatively explained by deploying the Born approximation. The $\Delta G_{solvation,\ Born}$ $(=-1/(2R_{TAML})\ [(q_{red}^2-q_{ox}^2)])$ term decreases along the same series due to the increase in the $(q_{red}^2-q_{ox}^2)$ term, in which $R_{TAML}$ is the constant effective radius of the TAML species and $q$ is the overall charge on the oxidized- and reduced TAML activators (see the Supporting Information). As a result, $\Delta G_{total} = \Delta G_{electronic} + \Delta G_{solvation}$ shows a non-monotonic dependence (Figure 4), the consequence of which is reflected in the $k_{II}$ vs. pH profile

A robust conclusion of the theoretical analysis is that the electronic and solvation contributions to the reduction free-energies for the $Fe^{IV}$ compounds change significantly and in the opposite directions upon deprotonation across the entire series. The electronic and solvation contributions nearly compensate for each other. Thus, the total oxidation power of the $Fe^{IV}$ species can either decrease with pH (if the electronic contribution dominates) or increase (if changes in the solvation terms are larger in magnitude). It is important to point out that both the electronic and solvation terms are computed by necessity using relatively imprecise theoretical models—TAML activators contain a transition metal and more than 20 heavy atoms, therefore significant computational errors are associated with the computed total reduction free-energies. Whereas the reactivities of *B* and *C* are predicted to be higher than those of *A* and *D*, which is in

  

agreement with experimental results, the reactivity of *C* appears to be lower (more positive free-energy of reduction) than that of *B*. The discrepancy can be due to the underestimation of electronic affinity energies for anionic compounds that are common in Hartree–Fock calculations used in the study. This theoretical analysis also explains why peroxidases, in contrast with small molecule peroxide activators, demonstrate a monotonic decrease in activity[14,25] as the pH is increased. In peroxidase enzymes, the heme group is immersed in a relatively non-polar protein environment. Thus, changes in the solvation contributions to the reduction free-energies are likely to be smaller than those for TAML activators. Changes in activity of heme-oxo intermediates of peroxidases on deprotonation of amino acid residues of the active site are thus likely to be dominated by the electronic contributions. When we were struck by the apparently counterintuitive ordering reactivity toward $[Fe(CN)_6]^{4-}$ reduction, we were assuming that the reactivity can be deduced entirely from the reduction potentials of the $Fe^{IV}$ compounds, which are related to $\Delta G_{total}$. We expect the oxidation of $[Fe(CN)_6]^{4-}$ to proceed through a simple outer-sphere electron-transfer mechanism with other parameters contributing to the control of the electron-transfer rate such as the solvent reorganization energy $\lambda$ with the donor/acceptor electronic coupling (in the contact configuration between $Fe^{IV}$ and $[Fe(CN)_6]^{4-}$) being similar across the *A*–*D* series.

This is the first in-depth study of the reactivity of the "Oxidized TAML" species. It is important to remember that the experiments "see" only the Compound II analogues in the TAML catalytic cycles with the assumption that Compound I analogues are also present and are reacting fast. The behavior has been studied over a wide pH range where we find no less than four Compound II mimics related to each other by acid–base equilibria, each exhibiting its own separate contribution to the overall process. The non-monotonic reactivity pattern with its counterintuitive elements, which are based on the relative electronic characters of the respective $Fe^{IV}$ complexes, can be explained by the presence of competing contributions from the electronic energy change and the solvation energy change to the overall free energy change for the redox process.

## Experimental Section

**General procedure for oxidation of ferrocyanide by $Fe^{III}$-TAML/$H_2O_2$**: In a typical experiment, appropriate volumes of the buffer, $K_4Fe(CN)_6$ and catalyst (**1a** or **1b**) stock solutions were added to a disposable polystyrene cuvette (1.5 mL) to attain the desired molar concentrations. The reaction was initiated by the addition of appropriate volume of $H_2O_2$. Initial reaction rates were measured by monitoring the formation of the product $K_3Fe(CN)_6$ at 420 nm ($\lambda_{max}$), at which $K_4Fe(CN)_6$ does not absorb light. The measured extinction coefficients of ferricyanide at this wavelength at pH 7, 10, and 12 are $960 \pm 10$, $980 \pm 10$, and $950 \pm 10\,M^{-1}cm^{-1}$, respectively, and are in agreement with a previously reported value.[14] The reaction rate for the uncatalyzed reaction (by $H_2O_2$ only) was subtracted from that of the catalyzed reaction ($Fe^{III}$–TAML + $H_2O_2$). See the Supporting Information for other details of the experimental procedures. The Hartree–Fock method and 6–311G(d,p) basis set was used for energy-optimization calculations with solvation effects accounted for within the polarizable continuum model (PCM).[26]

## Acknowledgements

Support is acknowledged from the Heinz Endowments (T.J.C.), the Institute for Green Science (T.J.C.) and Carnegie Mellon University (T.J.C.). S.K. thanks the R.K. Mellon Foundation for a Presidential Fellowship in the Life Sciences. M.A. thanks Carnegie Mellon University for Howard Hughes Medical Institute (HHMI) grant number 52006917. The authors thank Dr. Karla Arias for helpful discussions.

**Keywords:** acid-base equilibrium · bio-mimetic catalysis · iron · kinetics · oxidation

[1] A. Ghosh, D. A. Mitchell, A. Chanda, A. D. Ryabov, D. L. Popescu, E. C. Upham, G. J. Collins, T. J. Collins, *J. Am. Chem. Soc.* **2008**, *130*, 15116–15126.
[2] T. J. Collins, C. Walter, *Sci. Am.* **2006**, *294*, 82–90.
[3] F. Tiago de Oliveira, A. Chanda, D. Banerjee, X. Shan, S. Mondal, L. Que. , Jr., E. L. Bominaar, E. Münck, T. J. Collins, *Science* **2007**, *315*, 835–838.
[4] A. Ghosh, F. Tiago de Oliveira, T. Yano, T. Nishioka, E. S. Beach, I. Kinoshita, E. Münck, A. D. Ryabov, C. P. Horwitz, T. J. Collins, *J. Am. Chem. Soc.* **2005**, *127*, 2505–2513.
[5] D. L. Popescu, M. Vrabel, A. Brausam, P. Madsen, G. Lente, I. Fabian, A. D. Ryabov, R. v. Eldik, T. J. Collins, *Inorg. Chem.* **2010**, *49*, 11439–11448.
[6] A. Chanda, X. Shan, M. Chakrabarti, W. C. Ellis, D. L. Popescu, F. Tiago de Oliveira, D. Wang, L. Que. , Jr., T. J. Collins, E. Münck, E. L. Bominaar, *Inorg. Chem.* **2008**, *47*, 3669–3678.
[7] S. Kundu, J. V. K. Thompson, A. D. Ryabov, T. J. Collins, *J. Am. Chem. Soc.* **2011**, *133*, 18546–18549.
[8] D. Banerjee, PhD thesis, Carnegie Mellon University (USA), **2007**.
[9] W. C. Ellis, C. T. Tran, R. Roy, M. Rusten, A. Fischer, A. D. Ryabov, B. Blumberg, T. J. Collins, *J. Am. Chem. Soc.* **2010**, *132*, 9774–9781.
[10] N. Chahbane, D. L. Popescu, D. A. Mitchell, A. Chanda, D. Lenoir, A. D. Ryabov, K. W. Schramma, T. J. Collins, *Green Chem.* **2007**, *9*, 49–57.
[11] A. Chanda, A. D. Ryabov, S. Mondal, L. Alexandrova, A. Ghosh, Y. Hangun-Balkir, C. P. Horwitz, T. J. Collins, *Chem. Eur. J.* **2006**, *12*, 9336–9345.
[12] D. L. Popescu, A. Chanda, M. J. Stadler, S. Mondal, J. Tehranchi, A. D. Ryabov, T. J. Collins, *J. Am. Chem. Soc.* **2008**, *130*, 12260–12261.
[13] J. Sobkowski, *Roczniki Chemii* **1969**, *43*, 1729–1737.
[14] B. B. Hasinoff, H. B. Dunford, *Biochemistry* **1970**, *9*, 4930–4939.
[15] M. F. Zipplies, W. A. Lee, T. C. Bruice, *J. Am. Chem. Soc.* **1986**, *108*, 4433–4445.
[16] H. B. Dunford, *Heme Peroxidases*, Wiley-VCH, New York, **1999**.
[17] L. Q. Shen, E. S. Beach, Y. Xiang, D. J. Tshudy, N. Khanina, C. P. Horwitz, M. E. Bier, T. J. Collins, *Environ. Sci. Technol.* **2011**, *45*, 7882–7887.
[18] S. Kundu, A. Chanda, L. Espinosa-Marvan, S. K. Khetan, T. J. Collins, *Catal. Sci. Technol.* **2012**, *2*, 1165–1172.
[19] A. Chanda, S. K. Khetan, D. Banerjee, A. Ghosh, T. J. Collins, *J. Am. Chem. Soc.* **2006**, *128*, 12058–12059.
[20] D. Banerjee, A. L. Markley, T. Yano, A. Ghosh, P. B. Berget, E. G. Minkley, S. K. Khetan, T. J. Collins, *Angew. Chem.* **2006**, *118*, 4078–4081; *Angew. Chem. Int. Ed.* **2006**, *45*, 3974–3977.
[21] A. Ghosh, A. D. Ryabov, S. M. Mayer, D. C. Horner, D. E. Prasuhn, Jr., S. Sen Gupta, L. Vuocolo, C. Culver, M. P. Hendrich,

  

C. E. F. Rickard, R. E. Norman, C. P. Horwitz, T. J. Collins, *J. Am. Chem. Soc.* **2003**, *125*, 12378–12379.
[22] M. Oszajca, A. Franke, M. Brindell, G. Stochel, R. v. Eldik, *Inorg. Chem.* **2011**, *50*, 3413–3424.
[23] I. Spasojević, O. M. Colvin, K. R. Warshany, I. Batinić-Haberle, *J. Inorg. Biochem.* **2006**, *100*, 1897–1902.
[24] P. Hambright, P. B. Chock, *J. Inorg. Nucl. Chem.* **1975**, *37*, 2363–2366.
[25] M. L. Cotton, H. B. Dunford, *Can. J. Chem.* **1973**, *51*, 582–587.
[26] J. Tomasi, B. Mennucci, R. Cammi, *Chem. Rev.* **2005**, *105*, 2999–3093.

Received: May 11, 2012
Published online: July 24, 2012

  